

A Compact Narrow-Band Bandstop Filter Using Spiral-Shaped Defected Microstrip Structure

Jun WANG¹, Huansheng NING^{1,2}, Qingxu XIONG¹, Lingfeng MAO³

¹ School of Electronic and Information Engineering, Beihang University, Beijing, 100191, China

² School of Computer and Communication, University of Science and Technology Beijing, Beijing, 100083, China

³ Institute of Intelligent Structure and System, Soochow University, Suzhou, 215006, China

junwang@ee.buaa.edu.cn, ninghuansheng@buaa.edu.cn, qxxiong@buaa.edu.cn, mail_lingfeng@yahoo.com.cn

Abstract. A novel compact narrow-band bandstop filter is implemented by using the proposed spiral-shaped defected microstrip structure (SDMS) in this paper. Compared with other DMSs, the presented SDMS exhibits the advantage of compact size and narrow stopband. Meanwhile, an approximate design rule of the SDMS is achieved and the effects of the dimensions on the resonant frequency and 3dB fractional bandwidth (FBW) are analyzed in detail. Both the simulation and measurement results of the fabricated bandstop filter show that it has a 10 dB stopband from 3.4 GHz to 3.6 GHz with more than 45 dB rejection at the center frequency.

Keywords

Bandstop filter, defected microstrip structure (DMS), microstrip.

1. Introduction

To suppress an undesired signal closely located from the desired signal in the frequency spectrum, bandstop filters with narrow stopband, high performance and compact size are highly desirable in modern wireless applications. Recently, defected ground structure (DGS) has been provided a popular solution to address that need by taking advantage of the obvious stopband and slow-wave effect of the patterned structures [1], [2]. Various kinds of DGSs with high Q-factor have been proposed for the narrow-band bandstop filter design [3-5].

On the basis of DGS, defected microstrip structure (DMS) is developed by etching a uniform or non-uniform slit on the signal strip. Since the ground plane of DMS is integral, the DMS would be easier to integrate with other components compared with DGS. Moreover, the DMS features less crosstalk and electromagnetic interference (EMI) ground noise [6]. Some types of the DMSs have already been implemented in microwave applications, such as the T-shaped [7], [8], C-shaped [9] and M-shaped [10]. However, the physical understanding of the interaction between EM waves and the structure needs to be further investigated to provide a design rule. Moreover, the realiza-

tion of bandstop filter using DMS for more compactness and narrower band still remains challenging.

In this paper, a novel spiral-shaped DMS (SDMS) is proposed to obtain the narrow stopband and miniaturized size. Compared with the conventional spiral-shaped DGS (SDGS) [3], the patterned structure is etched in the signal strip and its orientation is parallel with the signal strip. Firstly, the SDMS and SDGS are simulated with the same dimensions to verify the above design concept. The SDMS and other presented DMSs in [8-10] are designed to resonate at the same frequency for compactness and stopband bandwidth comparison. Secondly, an approximate design rule of the SDMS is obtained, and the effects of the dimensions on the resonant frequency and 3 dB fractional bandwidth (FBW) are investigated. Finally, a narrow-band bandstop filter is designed, simulated and measured by cascading three SDMSs.

2. Spiral-Shaped Defected Microstrip Structure

The layout of the proposed SDMS is shown in Fig. 1(a), where the patterned spiral-shaped structure is etched along the signal strip. Here, we use the parameter

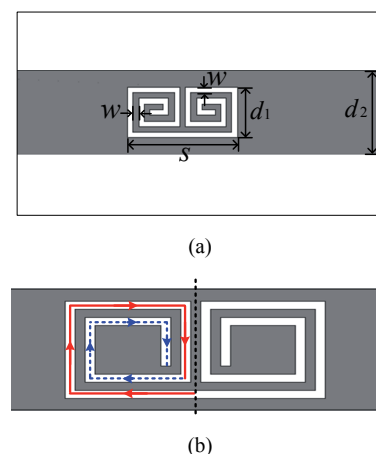


Fig. 1. (a) Layout of the proposed SDMS (top view). (b) Schematic diagram of the turn number $N = 2$ (each turn consists of four-sided slots).

Resonant Cell	Dimension Details (mm)	Occupying Width (mm)	Occupying Length (mm)	Occupying Area (mm ²)	3 dB Bandwidth (GHz)
T-shaped [8]	$b = g = 0.3, l = 20.8,$ $c = 3.2$	3.5	20.8	72.8	3.90
C-shaped [9]	$w1 = 0.65, w2 = 2.6, L1 = 11.5,$ $c1 = c2 = 0.3, g = 0.3$	3.2	11.5	36.8	0.81
M-shaped [10]	$a = 7.8, b = 0.53,$ $c = 0.3$	2.7	8.8	23.8	0.35
Spiral-shaped	$w = 0.3, d1 = 2.7,$ $N = 2.25, s = 6.3$	2.7	6.3	17.0	0.26

Tab. 1. Size and 3 dB bandwidth comparison of four shaped DMSs at the same resonant frequency of 4.0 GHz.

turn number N to describe the sided slots of SDMS and the definition of each turn is illustrated in Fig. 1(b). The width of the slot and the gap between adjacent parallel slots are chosen as the same value w .

Compared with the conventional SDGS [3], the configuration of the SDMS is to obtain a narrower stopband and lower resonant frequency. To demonstrate that, the SDMS and conventional SDGS with the same dimensions are simulated by the full-wave solver Ansoft HFSS. The substrate used in the simulations has a relative permittivity of $\epsilon_r = 2.55$ and a thickness of $h = 1.5$ mm. Fig. 2 shows the simulated S-parameters of both structures, where the resonant frequencies of the SDMS and the SDGS are at 4.0 GHz and 4.46 GHz respectively, and the 3dB bandwidths are 0.26 GHz and 1.15 GHz correspondingly. Therefore, the aforementioned design concept is validated. Moreover, the SDMS has no spurious resonance in the simulated frequency range and exhibits a pole located around 3.0 GHz in the reflection coefficient, which is useful for the high-performance bandstop filter realization.

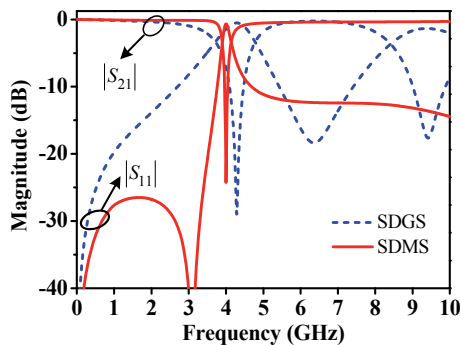


Fig. 2. Simulated S-parameters of SDMS and conventional SDGS with the same dimensions. ($w = 0.3$ mm, $d_1 = 2.7$ mm, $s = 6.3$ mm, $d_2 = 4.5$ mm, $N = 2.25$).

The SDMS and other shaped DMSs in [8-10] are designed to resonate at the same frequency of 4.0 GHz for compactness and 3 dB bandwidth comparison. The detailed dimensions of these structures are listed in Tab. 1 (the microstrip width of these structures is all set as 4.5 mm corresponding to a characteristic impedance of 50 Ω). All these structures are simulated with the transmission coefficient results shown in Fig. 3. As can be seen in this figure,

the structures all resonate at 4.0 GHz according to the design specifications. It is noted that the M-shaped DMS has an obvious spurious resonance near 8.5 GHz. From Tab. 1, we could find that the SDMS occupies the smallest circuit area, which is only 23.35 % of the T-shaped DMS and 71.43 % of the M-shaped DMS. Meanwhile, the SDMS has the narrowest 3 dB bandwidth of 0.26 GHz.

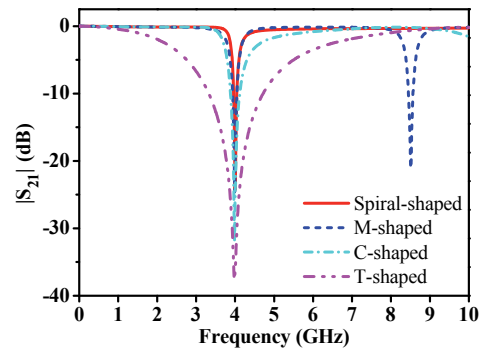


Fig. 3. Simulated transmission coefficients of different shaped DMSs at the same resonant frequency of 4.0 GHz.

Since the full-wave analysis cannot provide the direct correlation between the physical dimensions of the structure and the operated frequency, it is often necessary to obtain the design rule. The proposed SDMS can be regarded as a meandered slot line, thus, the resonant frequency f_r may be given approximately by the following expression:

$$f_r = \frac{c}{2L_{\text{slot}}\sqrt{\epsilon_{\text{eff}}^{\text{slot}}}} \quad (1)$$

where L_{slot} is the total length of meandered slot line, $\epsilon_{\text{eff}}^{\text{slot}}$ is the effective relative permittivity of the slot, c is the speed of the light in free space.

For the dimensions of the SDMS given in Fig. 2, the predicted resonance is located at 3.80 GHz, which is very close to the simulated resonance at 4.0 GHz. Hence, given a desired resonant frequency, we can use (1) to define the initial total length for a first design. The final design may be realized by adjusting the dimensions of the SDMS with the aid of full-wave simulation.

It is worth mentioning that the transmission response of the SDMS can be represented by a parallel RLC circuit and the 3 dB FBW can be approximately estimated as [12]:

$$FBW = \frac{\sqrt{2 - (1 + 2GZ_0)^2}}{2Z_0} \sqrt{\frac{L}{C}} \quad (2)$$

where $G = 1/R$, $GZ_0 \leq \sqrt{2} - 1/2$, L , C is the equivalent inductance and capacitance respectively which may be obtained using the expressions in [4], Z_0 is characteristic impedance of the microstrip line.

The effects of the dimensions on the resonant frequency and the 3 dB FBW are investigated to achieve a better understanding of the operating principle for the SDMS design. When the slot width w , the turn number N and the length of the SDMS s are changed respectively, the variations of the simulated resonant frequency and the 3 dB FBW and the calculated 3 dB FBW using (2) are plotted in Fig. 4, Fig. 5 and Fig. 6 correspondingly, which are concluded as follows:

- a) As w increases, it has insignificant contribution to the total length of the meandered slot line, thus, the variation of the resonance is not obvious based on (1). However, the 3 dB FBW increases rapidly due to the increased L , decreased G and C .

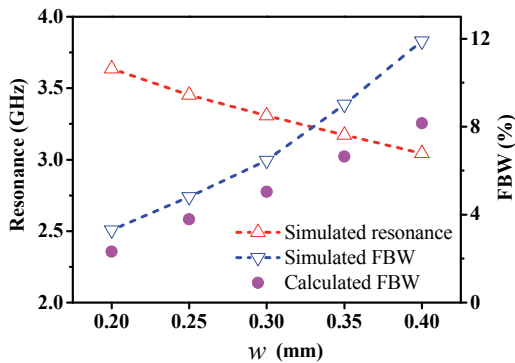


Fig. 4. Effects of the width w on the resonant frequency and 3 dB FBW ($N = 2.25$, $s = 7.2 \text{ mm} + 2w$).

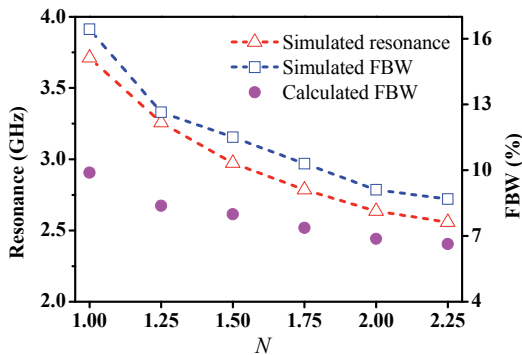


Fig. 5. Effects of the turn number N on the resonant frequency and 3 dB FBW ($w = 3.0 \text{ mm}$, $d_1 = 3.6 \text{ mm}$, $s = 7.8 \text{ mm}$).

- b) As N increases, the total length of the meandered slot line increases quickly, leading to the reduction of the resonant frequency. The 3 dB FBW decreases fast

when N increases at the initial stage resulted from the quickly increased C , and then the variation of the 3 dB FBW is relatively slower.

- c) As s increases, it will make a fast increase of the total length of the meandered slot line, resulting in the rapid reduction of the resonant frequency. The 3 dB FBW changes slowly because of the simultaneously increased L and C .

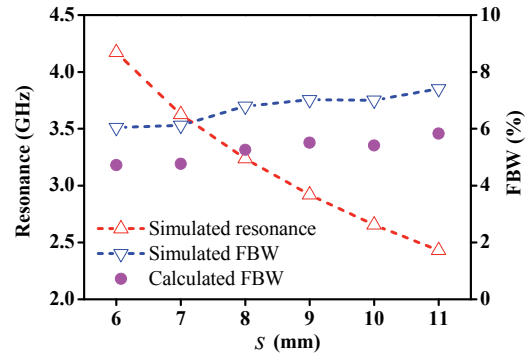


Fig. 6. Effects of the length s on the resonant frequency and 3 dB FBW ($N = 2.25$, $w = 0.3 \text{ mm}$, $d_1 = 2.7 \text{ mm}$).

Due to the approximation used in [12], the 3 dB FBW calculated by (2) has some difference with the actual simulated FBW in Fig. 4, Fig. 5 and Fig. 6. However, the trend of the 3 dB FBW change in the calculations is consistent with the simulations. Thus, the variation of the 3 dB FBW is explained qualitatively, which may be helpful for the structure design.

3. Narrow-Band Bandstop Filter Implementation

Based on the analysis of the SDMS above, a compact narrow-band bandstop filter is implemented by cascading three SDMSs along the signal strip and Fig. 7 shows its configuration. The distance between adjacent SDMSs is about a quarter of the guided wavelength at the resonant frequency. Here, the bandstop filter is designed to resonate at 3.5 GHz for suppressing the WiMAX radio interference.

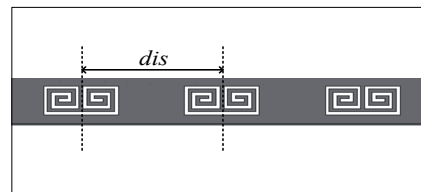


Fig. 7. Configuration of the bandstop filter (top view).

By using (1), the initial dimensions of the SDMS can be determined and the final design is obtained by the full-wave simulation. The optimal dimensions of the presented filter are as follows: $N = 2.25$, $w = 0.3 \text{ mm}$, $d_1 = 2.7 \text{ mm}$, $d_2 = 4.5 \text{ mm}$, $s = 7.3 \text{ mm}$, $dis = 12.5 \text{ mm}$. The designed bandstop filter is fabricated on Arlon Cuclad 250(tm) substrate with $\epsilon_r = 2.55$ and $h = 1.5 \text{ mm}$. Fig. 8 shows the

photograph of the fabricated filter and its simulated and measured results are plotted in Fig. 9, where a good agreement between the simulation and measurement is observed. Little discrepancy at the higher frequency range is mostly attributed to the effects the SMA connectors in the measurement. The center frequency of the stopband is at 3.48 GHz and the rejection level is more than 45 dB. The 10 dB rejection band is from 3.40 GHz to 3.60 GHz. Detailed data show that the measured insertion loss at the higher frequencies of the passband is within 1 dB.

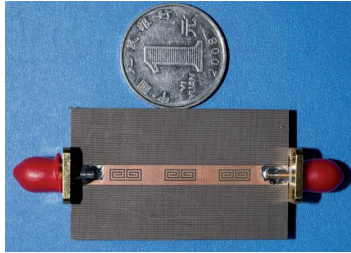


Fig. 8. Photograph of the fabricated bandstop filter.

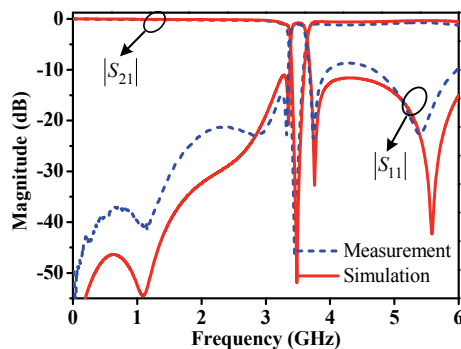


Fig. 9. Simulated and measured S-parameters of the fabricated narrow-band bandstop filter.

4. Conclusion

A compact narrow-band bandstop filter is realized by using the SDMS in this paper. The proposed SDMS has the minimal occupying area and the narrowest stopband compared with other DMSs at the same resonant frequency. An approximate design rule of SDMS is established from the perspective of meandered slot line. The variations of the resonant frequency and the 3 dB FBW against the dimensions of the SDMS are analyzed. Finally, a narrow-band bandstop filter is designed and fabricated by cascading three SDMSs. With good performance and compact size, the proposed filter can be easily integrated with other devices in wireless communication systems for enhanced performance.

References

[1] AHN, D., PARK, J.-S., KIM, C.-S., KIM, J., QIAN, Y., ITOH, T. A design of the low-pass filter using the novel microstrip defected ground structure. *IEEE Trans. on Microwave Theory and Techniques*, 2001, vol. 49, no. 1, p. 86-92.

[2] PARUI, S. K., DAS, S. Modeling of modified split-ring type defected ground structure and its application as bandstop filter. *Radioengineering*, 2009, vol. 18, no. 2, p. 149-154.

[3] KIM, C., LIM, J., NAM, S., KANG, K., PARK, J., KIM, G., AHN, D. The equivalent circuit modeling of defected ground structure with spiral shape. In *IEEE MTT-S International Microwave Symposium*. Seattle (USA), 2002, p. 2125-2128.

[4] WOO, D., LEE, T., LEE, J., PYO, C., CHOI, W. Novel U-slot and V-slot DGSs for bandstop filter with improved Q factor. *IEEE Trans. on Microwave Theory and Techniques*, 2006, vol. 54, no. 6, p. 2840-2847.

[5] HUANG, S.-Y., LEE, Y.-H. A compact E-shaped patterned ground structure and its application to tunable bandstop resonator. *IEEE Trans. on Microwave Theory and Techniques*, 2009, vol. 57, no. 3, p. 657-666.

[6] KAZEROONI, M., CHELDAVI, A. Simulation, analysis, design and applications of array defected microstrip structure (ADMS) filters using rigorously coupled multi-strip (RCMS) method. *Progress in Electromagnetics Research, PIER*, 2006, vol. 63, p. 193-207.

[7] TIRADO-MÉNDEZ, J. A., JARDÓN-AGUILAR, H., et al. A proposed defected microstrip structure (DMS) behavior for reducing rectangular patch antenna size. *Microwave and Optical Technology Letter*, 2004, vol. 43, no. 6, p. 481-484.

[8] ZHANG, S., XIAO, J.-K., WANG, Z.-H., LI, Y. Novel low pass filters using a defected microstrip structure. *Microwave Journal*, 2006, vol. 49, p. 118-128.

[9] FALLAHZADEH, S., TAYARANI, M. A new microstrip UWB bandpass filter using defected microstrip structures. *Journal of Electromagnetic Waves and Applications*, 2010, vol. 24, p. 893 to 902.

[10] LA, D., LU, Y., SUN, S., LIU, N., ZHANG, J. A novel compact bandstop filter using defected microstrip structure. *Microwave and Optical Technology Letter*, 2011, vol. 53, no. 2, p. 433-435.

[11] JANASWAMY, R., SCHAUBERT, D. H. Characteristic impedance of a wide slotline on low-permittivity substrates. *IEEE Trans. on Microwave Theory and Techniques*, 1986, vol. 34, no. 6, p. 900-902.

[12] KIM, H.-M., LEE, B. Bandgap and slow/fast-wave characteristics of defected ground structures (DGSs) including left-handed features. *IEEE Trans. on Microwave Theory and Techniques*, 2006, vol. 54, no. 7, p. 3113-3120.

About Authors ...

Jun WANG was born in 1987. He is currently working towards the Ph.D. degree in Electronic Engineering at Beihang University. His research interest focuses on the design and implementation of novel planar microwave passive circuits.

Huansheng NING received the B.S. degree from Anhui University in 1996 and Ph.D. degree in Beihang University in 2001. He is a professor in the School of Computer and Communication, University of Science and Technology Beijing, China. His current research focuses on Internet of Things, electromagnetic sensing and computing.

Qingxu XIONG received the Ph.D. degree in Electrical Engineering from Peking University, Beijing, China, in 1994. From 1994 to 1997, he worked in the Information

Engineering Department at Beijing University of Posts and Telecommunications as a Postdoctoral Researcher. He is currently a Professor in the School of Electrical and Information Engineering at Beihang University, Beijing, China. His research interests include scheduling in optical and wireless networks, performance modeling of wireless networks, satellite communication.

Ling-Feng MAO received the Ph.D. degree in microelectronics and solid state electronics from the Peking University, Beijing, P. R. China, in 2001. He is a professor in Soochow University. His research activities include modeling and characterization of semiconductor devices and circuits, the fabrication and modeling of integrated optic and microwave devices and circuits.